REDISTRIBUTION OF CARBON FROM SILICON BY ELECTRON BEAM MELTING

H. M. N. KHAN ASGHAR[abc], M. S. SHIFA[f], Z. A. GILANI[c*], P. WANG[a,b],
J. U. REHMAN[c], M. N. ANJUM[d], M. N. USMANI[e], Y. TAN[a,b], S. SHI[a,b],
D. JIANG[a,b], S. QIN[a,b]
[a]*School of Materials Science and Engineering, Dalian University of Technology,
Dalian 116023, China*
[b]*Key Laboratory for Solar Energy Photovoltaic System of Liaoning Province,
Dalian 116023, China*
[c]*Department of Physics, Balochistan University of Information Technology,
Engineering & Management Sciences, Quetta 87300, Pakistan*
[d]*Department of Physics, the Islamia University of Bahawalpur*
[e]*Department of Physics, Bahauddin Zakariya University, Multan, Pakistan.*
[f]*Department of Physics, Govt College University, Faisalabad, Pakistan*

To investigate the carbon and silicon carbide flow behavior during the electron beam melting (EBM) process, 100 gram of multi-crystalline silicon with the contamination of SiC was melted in an electron beam furnace for five minutes. The EBM Experiment performed in the contaminated sample caused the redistribution of the impurities. The Electron Probe Microstructure Analysis (EPMA) microscopy, SEM and EDS have been utilized to experimentally observe the redistribution pattern. After EBM, carbon enriches in the form of SiC at the bottom of the ingot but not in the center. The results show that there is great temperature gradient existing in the melt during EBM, so the melt near copper crucible shows low temperature and bad fluidity. Carbon in silicon melt flows with the melt, precipitated and gathered in this area so that it is separated due the segregation of the impurities alongside the bottom of the sample through EBM technique.

1. Introduction

Modern research on high efficiency, low priced, minimum zero level infectivity Photovoltaic (PV) cells with an extensive life-time has a promising future. In the last 20 years, the PV industry around the modern world has enjoyed a very high growth rate [1]. In contemporary period, the consumption of solar grade silicon (SoG-Si) is increasing day by day with a quick improvement of photovoltaic cell industry [2, 3]due to the increasing demand for clean and sustainable energy resources, intensified power consumption rate with progressing economy, and the shortage of natural energy resources on the earth.

Out of many available PV materials and technologies, a majority of commercial solar cells are based on crystalline silicon materials. Metallurgical grade silicon (MG-Si) has been considered as a feedstock to fabricate high quality multicrystalline silicon ingots directly by refining impurities [4]. MG-Si to SoG-Si provides with the fundamental groundwork for further development of photovoltaic industry [5-8].

As a last step of metallurgical process, pure silicon is loaded in a quartz (SiO2) crucible where it melts and reacts, inducing the carbon contamination due to the graphite heater inside the chamber. The presence of carbon degrades the electrical performance of silicon solar cells because of its interaction with Si to form Si-C complexes, and with carbon to form C-O complexes, and

---

[*]Corresponding author: zagilani2002@yahoo.com

segregating as oxide etc. carbon content for solar grade silicon should be less than 5 ppmw and the minority carrier lifetime should be more than 2 μs [9, 10]. Solidification mechanism in silicon casting ingot production is achieved through directional solidification. During this processing, a crucible of SiO_2 is internally polished with Si_3N_4 to prevent a bulk quantity of O_2 into the casted ingot. Meanwhile, O_2 and N_2 enter from the crucible contact areas and contaminate the sides with oxygen whereas upper part is contaminated with carbon and carbon flows towards the edges. The incorporation of oxygen and carbon around ingot-crucible contact areas causes 30% of the ingot to go into wastage [11, 12]. In China, about 120,000 tons of this kind of material is wasted every year.

The removal of oxygen from titanium alloy and from silicon by electron beam melting (EBM) has been reported [11, 13] but redistribution of carbon in the silicon melt by EBM is a different idea [14-16].EBM is characterized by high vacuum and high temperature. The EBM has been widely applied to refractory, reactive metals and is now used for purifying materials, specifically for impurities with high vapor pressure [17, 18].

In this research, an experiment was carried out to remove the content of carbon in silicon ingot after electron beam melting the system was not shut down for 5 more minutes to allow better redistribution of carbon. In order to clarify the removal mechanism of carbon, the distribution of carbon and the kinetic behavior of carbon from the melt free surface were investigated. The morphology of ingot was examined using the scanning electron microscopy (SEM) and energy dispersive spectroscopy (EDS). The flow mechanism of carbon and silicon was also discussed.

2. Experimental

The silicon samples were extracted from the top of a casted ingot, where the material presents the major contamination with carbon (up to 1.49% averagely) in the form of SiC and Si_3N_4. Before melting by electron beam, the sample was properly washed in alcohol by a supersonic wave cleaner in order to remove possible solid residues. For this experiment, 100g silicon was placed in a water cooled copper crucible. The chamber and the electron beam gun were evacuated to less than 5.0×10^{-2} Pa and 5.0×10^{-3} Pa respectively; the filament and cathode were then pre-heated. Later, the melting process was performed. The electron beam with a power of 9kW was irradiated on the surface of the silicon until it was melted. Once silicon was melted completely, it was left for five minutes, and then electron beam was stopped instantaneously after the molten pool was held for a certain time. The silicon solidified in a short time and was removed from the crucible after cooling for 30 min. The carbon and Nitrogen content levels were determined by the Elemental Analyzer. The melting parameters are shown in Table 1.

Table 1. Melting parameters during EBM experiment

Melting Parameters	Value
Refining time(min)	5
Melting power(kW)	9
Chamber pressure(Pa)	$5.0 \times$ 10-2
Gun pressure (Pa)	$5.0 \times$ 10-3
Irradiation pattern	Circular
Scanning frequency (Hz)	10

3. Analysis of carbon contaminated silicon before Electron beam melting (EBM) treatment

3.1. Impurities of carbon and nitrogen contents in raw Si

The sample used for electron beam melting was taken from the top of the casted ingot. During casting process, the sample was in SiO_2 crucible and around the crucible, graphite heaters were used so the carbon concentration was high and silicon was contaminated with carbon, oxygen

and nitrogen. During casting process, Si_3N_4 internally polished SiO_2 crucibles were used to prevent the bulk entrance of oxygen into the ingot. When casted ingot solidified in the crucible, the silicon compounds with oxygen, carbon and nitrogen were observed. Oxygen Removal from silicon ingot process has already been discussed in our previous research. In this research we will contain ourselves about carbon and nitrogen compounds with silicon. It was also observed that the entire top surface of casted ingot was contaminated with SiC and Si_3N_4 and top surface of casted ingot also removed like sides. The flow of carbon was very effective in that period. The carbon moves towards the sides and edges of the molten pool resulting in almost 13% carbon concentration in the form of SiC and, in top, more than 9% of nitrogen in the form of Si_3N_4.

Table 2.Pickling statistical analysis of 5 silicon samples

Description	1	2	3	4	5
Before pickling Si+ insoluble (g)	6	6	6	6	6
Insoluble (g)	0.085	0.062	0.105	0.091	0.103
Insoluble %	1.42	1.03	1.75	1.52	1.72
Average %			1.49		

Five samples of Si (contaminated with insoluble impurities), each weighing 6 grams, were extracted from the top surface of cast-ingot (casted ingot). The samples were pickled with a mixture of hydrofluoric acid and nitric acid (the ratio of HF to HNO_3 3:1); causing the Si to dissolve in the mixture and leading to the separation of the insoluble impurities. The weights of impurities consisting of SiC and Si_3N_4 have been presented in Table 2, from where it can be inferred that they account for around 1.49 wt % on average. The individual elements of the powder impurities for the samples were investigated using elemental analyzer as shown in table 3, with a result that C accounts for 13% whereas N constitutes 9.07 % in average. From the elemental analyzer, some hydrogen contents also observed. But it is not our major concern in this research. All these impurities in table 3 are before the EBM treatment.

Table3. Results ratios of impurities element

impurities	C%	N%	H%
1	14.25	8.413	0.005
2	13.78	7.981	0.016
3	12.23	6.047	0.010
4	14.67	9.365	0.021
5	7.596	12.91	0.009

3.2 Microstructure analysis of impurity contents in raw Si

During casting, directional solidification of multicrystalline silicon ingots for the preparation of solar cells, the concentration of carbon and nitrogen contents of impurities in the silicon melts with the progression of solidification due to their relatively low segregation coefficients. Due to super saturation of carbon and nitrogen in silicon melt, SiC and Si_3N_4 inclusion are formed. In Figure1 a microstructure analysis of SiC was studied, a piece of multicrystalline silicon was selected from a casted silicon ingot and cut out from industrial level multicrystalline silicon ingot prepared through directional solidification method. The distribution of SiC inclusions was observed.

Element	Mass%	Atomic%
C	28.70	48.49
Si	71.30	51.51

Element	Mass%	Atomic%
C	16.94	23.32
N	44.03	51.97
O	3.91	4.04
Si	35.12	20.68
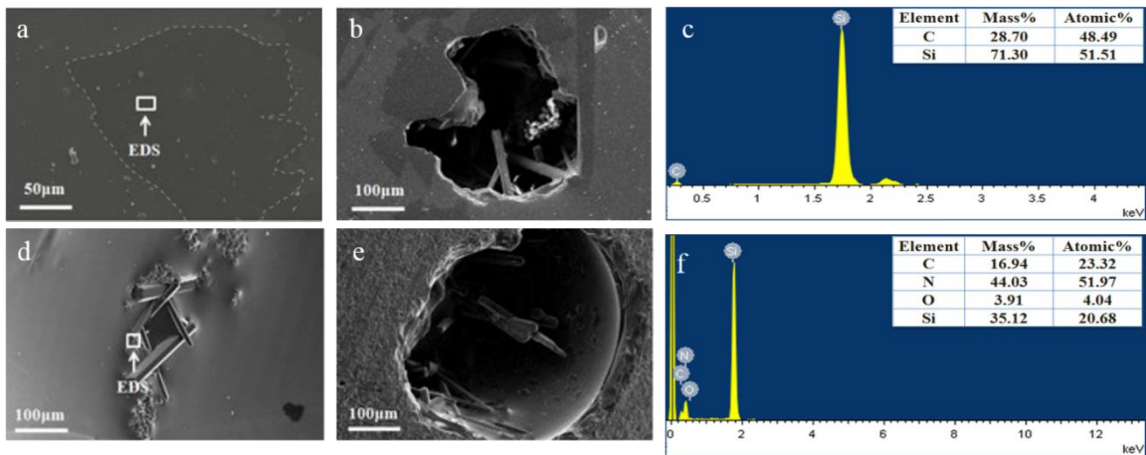
Fig. 1. a, b Microstructure of SiC in silicon raw material, c ,EDS analysis of the selected spot in Si raw material, d, e Microstructure of Si_3N_4 in silicon raw materialf, EDS analysis of the selected spot in silicon raw material

The presence of SiC inclusions generated high density of dislocations in multicrystalline silicon, and sometimes can be introduced pores into multicrystalline silicon. Morphologies and characteristics were also investigated. These results will have great interest for photovoltaic industrial researcher. In Figure 1(a) three different visions can be observed, there some white spots and two dark gray and light gray areas also observed. White spots indicate other impurities and light gray area represents silicon and dark gray area represents SiC, similarly another spot was selected in Figure 1(b) for the observations of SiC inclusions and some pores and rods like fiber were also observed. For further investigation a spot is selected from a dark region which is pointed out in Figure 1(a) and EDS analysis is presented for elemental investigation which is shown in Figure 1(c). The results showed it dark area was formed by SiC and the contents of carbon and Silicon were 28.70%, 71.30% by weight and 48.49%, 51.51% by atomic respectively.

The SEM analysis in Figure 1(d,) showed partially etched top surface area from multicrystalline silicon ingot where like a fiber rods were observed formed by Si3N4 and in neighbors some spots of SiC also observed. These pores of the rods were embedded in matrix form. While in Figure 1(e) showed partially etched multicrystalline silicon wafer with wire-sawing defects on its surface containing SiC and Si3N4 inclusions.

The foreign inclusions were exposed from the multicrystalline matrix and can be clearly observed in Fig. 1(d). Particles or spots showed the presence of SiC. Some Si_3N_4 rods protrude out from SiC particles. This implies that Si_3N_4 rods can act as a nucleation site for SiC growth. As shown in magnified SEM micrograph in Figure 1(e) the process revealed that the SiC particles embedded within multicrystalline silicon. The presence of SiC and Si_3N_4 inclusions can sometimes result in the formation of pores in the directionally solidified multicrystalline silicon. It was also interesting that Si_3N_4 rods are hollow and it was reported earlier in the silicon melt N_2 atmosphere [19, 20].

A selected area for EDS analysis and for elemental investigation is shown in Figure 1(f). EDS results showed that in the elemental analysis of SiC and Si_3N_4 the weight contents of carbon, nitrogen, oxygen and silicon were 16.94%, 44.03%, 3.915% and 35.12% by and of atomic percentage was 23.32%, 51.97%, 4.04% and 20.68% respectively were observed. Grain boundaries in multicrystalline materials are usually the localities that are bound with various impurities so foreign inclusions are preferentially present in grain boundaries in order to know whether SiC or Si_3N_4 inclusions in directionally solidified multicrystalline are also preferentially located in grain boundaries.

4. Experimental results and discussion of EBM treated silicon

4.1 Morphologies of the silicon ingot after the EBM process

100 g silicon melted ingot was investigated after EBM treatment from the barren of casted ingot from the top surface from the multicrystalline silicon. The morphologies of the silicon ingot and the cross sectional are shown in Figure 2. Weight loss of silicon ingots was recorded after the EBM process. The distributions of the impurities content were investigated by EPMA. Ingots were cut along the center line and morphologies of the cross sections were observed for the analysis of impurities distribution in the silicon as evident from Figure 2.

Fig.2.Morphologies of the silicon ingot and the cross section

4.2. Distribution of carbon content after the EBM process

Inclusions flow was observed towards to the bottom during investigation of five different lattice cut pieces of ingot and it was significantly reduced during melting of five minutes duration flowing down to bottom. Figure 3 (a) is from the central part top to bottom and less impurities are observed as compared to the bottom Figure 3(b) is from top of the free from SiC and Si_3N_4 silicon ingot can be observed and Figure 3(c), (d) and (e) are from the bottom part of the sample. In all figures related to bottom invert coloring rods, spots and inclusions are the impurities and most part of them was observed towards the bottom of the sample. So far the EBM method can be considered as most effective and efficient process to redistribute carbon compounds from silicon. Spots and rods inclusions are related to the SiC and Si_3N_4 respectively according to our last analysis and impurities can be collected from the sides or bottom of the solidified ingot or from the of the silicon melt due to the water cooled copper crucible.
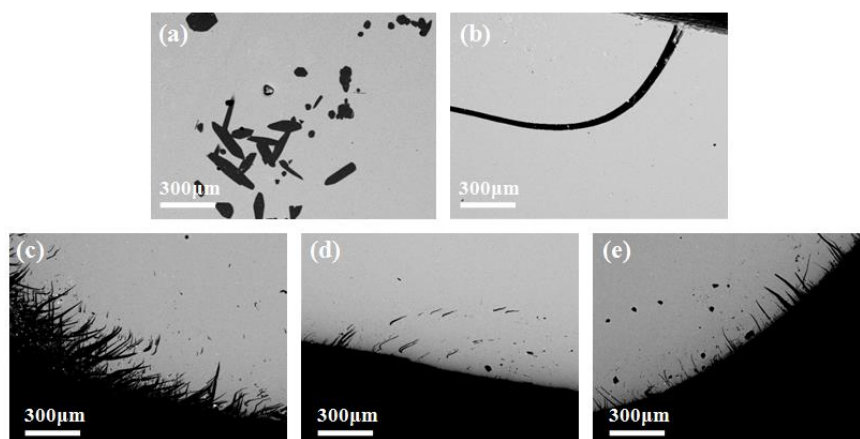
Fig.3.Inclusions distribution in silicon ingot after EBM treatment: (a) position 1;
(b) position 2; (b) position 3; (b) position 4; (b) position 5

The carbon atoms are transported onto the melt surface and react with the surface silicon atoms to produce SiC during the melting process. Following that resultant SiC flow from the melt pool to the bottom of the melt pool which is regarded as a main mechanism of the distribution for

carbon flow[21] as shown in Figure 4. Marginal distribution of impurity elements analysis is shown in Figure 4(a). Here in Figure 4four impurities tests were conducted for silicon, carbon, nitrogen and oxygen observed the results. It is taken from the bottom of the sample. In Figure 4(b) silicon distribution test all yellow or red spots shows the majorities of silicon and some green and blue areas shows the presence of impurities and in Figure 4 (c) is shown carbon distribution test in this image red spots or regions showed the carbon presence rest of areas silicon in Figure 4 (d) and (e) were about the distribution of nitrogen and oxygen from these images it can be observed obviously blue areas which shows the absence of nitrogen and oxygen. It is also observed that the distribution of carbon is only towards the sides or edges, central part are of silicon ingot is free of contaminated from impurities.
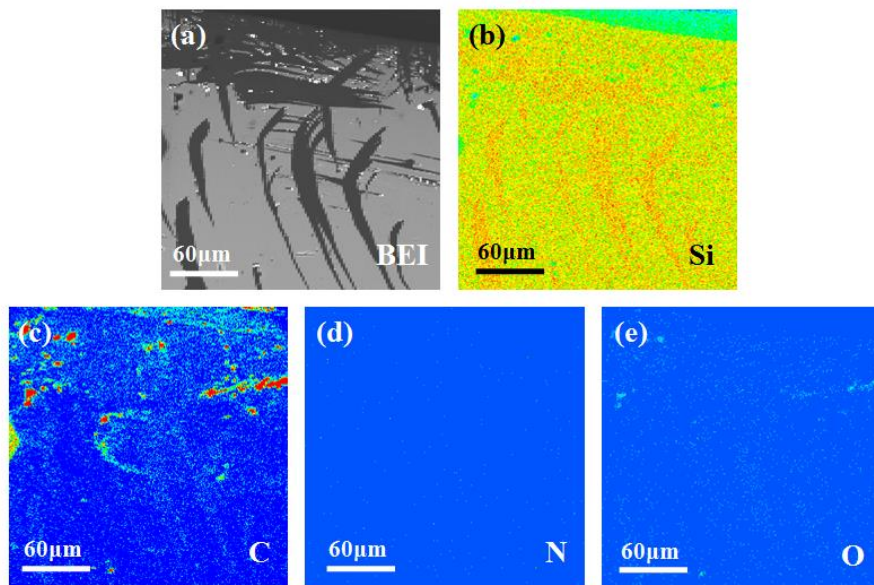
Fig.4. Elemental distribution analysis of the bottom: (a) BEI; (b) Si; (c) C; (d) N; (e) O

Selected surface and inner area of sample was analyzed for the massive distribution of impurities elements by EPMA as shown in Figure 5 (a). Light gray area indicates the silicon and dark gray areas or spots show the presence of impurities. Further investigation of massive distribution of impurities of in silicon ingot was made by keeping in to test. In Figure 5 (b) dark blue areas showed less presence of silicon in this region and similarly in Figure 5(c) light green area showed less magnitude of carbon. Moreover, in Figure 5 (d) some whitish blue regions indicated the presence of nitrogen and in the last Figure 5(e) almost has no oxygen in this region.
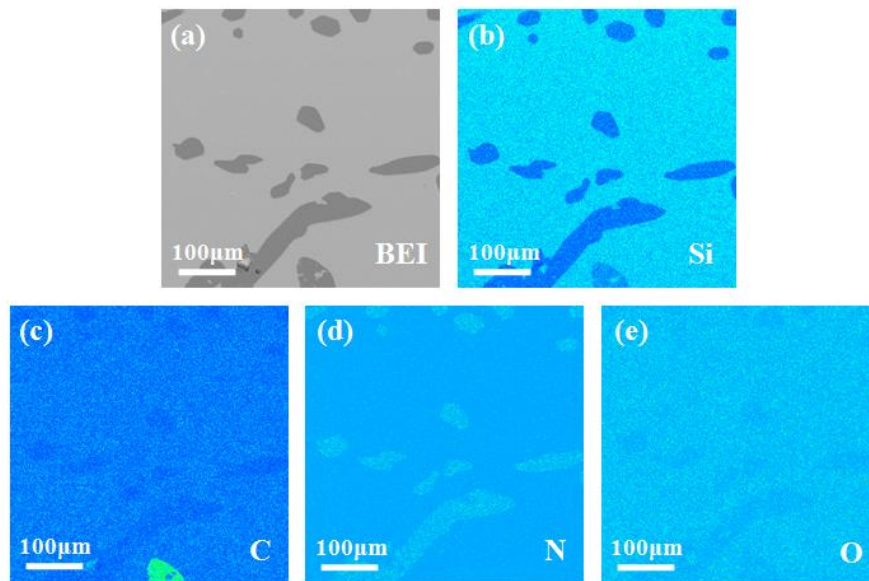
Fig.5. Elemental distribution analysis of central part: (a) BEI; (b) Si; (c) C; (d) N; (e) O

5. Theoretical Discussion

5.1. Melt Temperature during EBM Process

Redistribution behavior of carbon in the silicon melt is considered to be closely related to the temperature of the melt, it is necessary to obtain the temperature distribution in the melt during EBM. Because of the local overheating during EBM, the temperature of electron beam scanning area is beyond thermocouple temperature range in order to prevent the deposition of silicon on lead glass, a steel plate with high rotation speed was used in the viewing window, and the surface temperature of the melt will not be accurately measured by infrared pyrometer through the observation window. Therefore, this part applies the computer simulation method to obtain the temperature distribution of the silicon melt.

During EBM, electrons emitted by the electron beam gun bombard the surface of silicon materials. Then, the kinetic energy of the electrons is transformed into heat energy to melt the silicon materials. A silicon ingot is considered in the mathematical model to obtain the position of the solid-liquid interface during EBM, at the beginning of melting, electron beam direct role of regional temperature rises first, then heat the surrounding silicon uptake and transport to the bottom. Upon reaching steady state, occurs in close to a water-cooled copper crucible where lower temperatures does not melt zone, which is due to the water-cooled copper crucible is close to the heat having a high thermal conductivity of copper material absorbed away by the cooling water circulation, leading to the temperature of the region is significantly lower than the temperature in other areas. At the same time it can be observed in addition to the higher electron beam direct heating effect of the annular zone temperature, the other regions due to the strong water-cooled copper heat capacity, so that other areas of heat loss faster, lower temperatures in the region, so the internal temperature distribution of the silicon melt is not uniform, there is a large temperature gradient as shown in Figure 6.
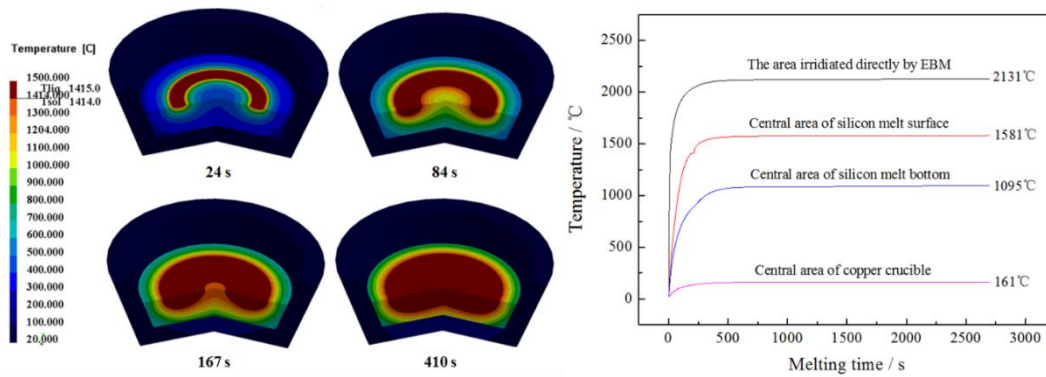
Fig.6. Four different stages of temperature during EBM from initial stage to maximum b. Four different points of temperature during EBM from outside crucible, inside surface of crucible, center of the sample and outer surface of the sample

From Fig.6 in the graph, the temperature of outside central part of crucible was observed 161 ℃.It was due to the water cooling system while the temperature of inside surface of crucible was observed 1095 ℃ but at this temperature silicon could not be melted and next point was central part of the sample where temperature was 1581 ℃ and the outer surface of the sample temperature was observed 2131 ℃ and at this temperature silicon can be melted. So it is revealed that at the bottom of the Cu crucible silicon cannot be melted due to water cooling mechanism and SiC and Si_3N_4 can migrate from top to bottom and the viscosity will be high and solubility will be low.

5.2. Melt Viscosity

From Fig.7 it is obviously observed that viscosity is the function of time and during silicon refining the operating temperature remain between melting temperature of Si which is 1687 K to 2500 K.

Using the formula for calculating the viscosity as:[22]

$$\log \eta \, (mPa \cdot s) = -0.727 + 819/T \tag{1}$$

At temperature 1687 K the viscosity was observed 16.311 mPa.s and it is found continuously with the increasing temperature the values of viscosity decreasing until at 2000 K the viscosity was 11.34 mPa.s.
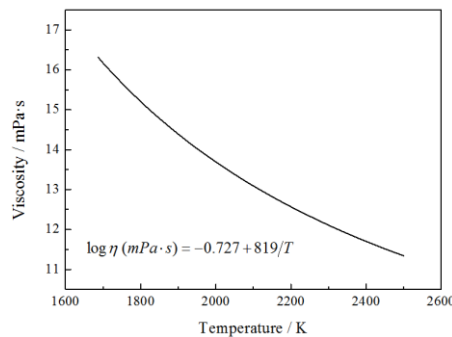
Fig.7. Viscosity is the function of temperature

5.3. Existing State of Carbon in Silicon Melt

Carbon content in elemental form is less than1.49% in ingot and from phase diagram as shown in From Figure 8, during EBM the temperature reaches almost 1800 ℃ in this temperature silicon turns into liquid form and SiC cannot remain in solid form. From the study of phase diagram, it is found SiC can be decompound into elemental form when temperature is more than 1500℃.So it is clear that carbon formed compound with silicon in when the temperature of silicon melt is a little more than the melting point. SiC can be precipitated in the low temperature melt area. Only silicon melt and carbon atoms exist when the temperature of silicon melt is far larger than the melting point, so SiC can be dissolved when it flows from the low temperature melt area to the high temperature melt area.

For understanding the solubility behavior of impurities like carbon in the silicon melt using the formula of solubility as:

$$C(T) = 839.4 \exp(-19856/T) \tag{2}$$
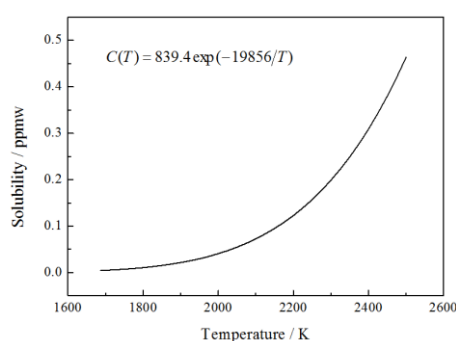
Fig.8. Solubility of carbon in silicon melt is the function of temperature

The solubility of an impurity is defined as the maximum concentration that can be dissolved in the lattice at a given temperature. The solubility depends exponentially on the temperature according to the above equation (1). As shown in Figure 8, the solubility decreases drastically towards the room temperature, hence during cooling down process like during ingot growth the dissolved metals become increasingly supersaturated. Same behavior of carbon in silicon melt was observed using equation (2). But the difference between nitrogen and carbon is less soluble then nitrogen in same temperature. Nitrogen solubility is sharply increased as compared to carbon after 2000 K.

5.4. Redistribution Mechanism of Carbon in Silicon

Fig.9 depicts the flow mechanism of SiC into the silicon ingot. As we know, graphite heaters are used during casting process. Keeping in mind all previous discussions and tests observations including theoretical, simulated, literature survey and experimental results that carbon is introduced due to graphite heaters and reacts with silicon melt hence forming SiC. Furthermore, SiC flows towards the bottom therefore bottom is more contaminated with SiC as compared to the center and the top surface area.
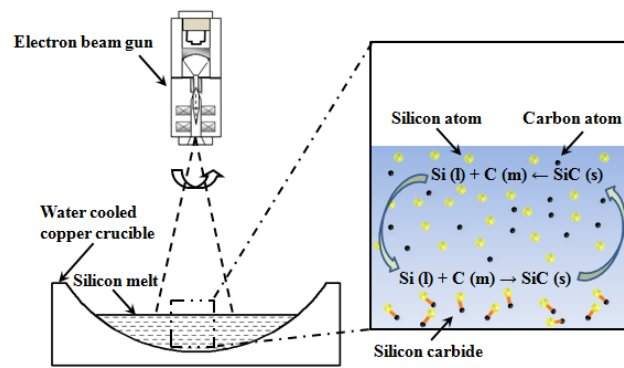
Fig.9. Mechanism of carbon flow towards the bottom of the silicon ingot

6. Conclusion

Carbon and Nitrogen have been observed as the constituent elemental impurities in the contaminated Si sample. To investigate the carbon flow behavior during the electron beam melting (EBM) process, 100 gram of multi-crystalline silicon was melted in an electron beam furnace for five minutes. The Carbon and Nitrogen content levels were determined by "Elemental Analyzer" before and after electron beam melting. The Electron Beam Melting (EBM) Experiment performed in the contaminated sample caused the redistribution of the impurities along bottom of the sample. The EPMA microscope has been utilized to experimentally observe the redistribution pattern of these impurities. Further, investigations with SEM and EDS confirmed that the impurities in compound forms are Si_3N_4 and SiC.

It is significant to note that the Silicon Nitride has a rod shaped microstructure whereas Silicon Carbide has a granular shaped morphology. In this research, silicon from the top of the casting ingot with high carbon content was melted and refined using EBM to investigate the migration behavior of carbon impurity in molten silicon. An important phenomenon was found that the carbon compounds content in silicon redistributed rapidly within the time range of approximately five minutes after completely melting. Carbon enriched in the form of SiC in the bottom of the ingot but not in the center. The results show that there is great temperature gradient existing in the melt during EBM, so the melt near copper crucible show low temperature and bad fluidity. Carbon in silicon melt flowed with the melt, precipitated and gathered in this area so that it was separated. With the segregation of the impurities along the bottom of the sample through EBM technique, the Si sample at other locations are obtained in pure form; thus implying that this purification technique could have potential application in the silicon based industries or Solar PV cell industries.

References

[1] H.M.N.U.K.[1] X.F. Qi, Q.H. Yu, W.H. Zhao, X.Q. Liang, J. Zhang, L.J. Liu, Sol Energ Mat Sol C, 130 (2014) 118-123.
[2] T. Matsui, M. Kondo, Sol Energ Mat Sol C, 119 (2013) 156-162.

[3] H.M.N.U.K. Asghar, Z.A. Gilani, M.S. Awan, I. Ahmad, Y. Tan, Arabian Journal for Science and Engineering, 40 (2015) 263-268.

[4] G. Coletti, Prog Photovoltaics, 21 (2013) 1163-1170.

[5] J.Y. Kwon, D.H. Lee, M. Chitambar, S. Maldonado, A. Tuteja, A. Boukai, Nano Letters, 12 (2012) 5143-5147.

[6] J.Y. Huang, C.Y. Lin, C.H. Shen, J.M. Shieh, B.T. Dai, Sol Energ Mat Sol C, 98 (2012) 277-282.

[7] N. Khedher, M. Hajji, M. Bouaicha, M.F. Boujmil, H. Ezzaouia, B. Bessais, R. Bennaceur, Solid State Communications, 123 (2002) 7-10.

[8] X.P. Li, Y.J. Xiao, J.H. Bang, D. Lausch, S. Meyer, P.T. Miclea, J.Y. Jung, S.L. Schweizer, J.H. Lee, R.B. Wehrspohn, Adv Mater, 25 (2013) 3187-3191.

[9] Y. Kato, K. Hanazawa, H. Baba, N. Nakamura, N. Yuge, Y. Sakaguchi, S. Hiwasa, F. Aratani, Tetsu to Hagane-Journal of the Iron and Steel Institute of Japan, 86 (2000) 9-16.

[10] J. Safarian, G. Tranell, M. Tangstad, Technoport 2012 - Sharing Possibilities and 2nd Renewable Energy Research Conference (Rerc2012), 20 (2012) 88-97.

[11] H. Noor Ul Huda Khan Asghar, S. Shi, D. Jiang, Y.I. Tan, Bull Mater Sci, 38 (2015) 1429-1433.

[12] H.M.N.U.K. Asghar, Y. Tan, S. Shi, D.C. Jiang, S.Q. Qin, J. Liao, S.T. Wen, W. Dong, Y. Liu, Appl Phys a-Mater, 115 (2014) 753-757.

[13] M. Werner, K. Scheerschmidt, E. Pippel, C. Funke, H.J. Moller, Microscopy of Semiconducting Materials 2003, 0 (2003) 65-68.

[14] T. Ikeda, M. Maeda, Isij Int, 32 (1992) 635-642.

[15] J.C.S. Pires, A.F.B. Braga, P.R. Mei, Sol Energ Mat Sol C, 79 (2003) 347-355.

[16] S. Qin, D. Jiang, Y. Tan, P. Li, P. Wang, S. Shi, Vacuum, 121 (2015) 207-211.

[17] S. Kashu, K. Watanabe, M. Nagase, C. Hayashi, Y. Yoneda, Journal of the Electrochemical Society, 128 (1981) 2453-2460.

[18] K. Sakamoto, K. Yoshikawa, T. Kusamichi, T. Onoye, Isij Int, 32 (1992) 616-624.

[19] N. Chen, B. Liu, S. Qiu, G. Liu, G. Du, Mat Sci Semicon Proc, 13 (2010) 231-238.

[20] R. Grun, J Cryst Growth, 46 (1979) 143-146.

[21] W. Ma, C.C. Lim, T. Saida, H. Okamoto, Y. Hamakawa, Sol Energ Mat Sol C, 34 (1994) 401-407.

[22] Y. Sato, Y. Kameda, T. Nagasawa, T. Sakamoto, S. Moriguchi, T. Yamamura, Y. Waseda, J Cryst Growth, 249 (2003) 404-415.